IEEE Access
Multidisciplinary ⋮ Rapid Review ⋮ Open Access Journal

Received August 6, 2021, accepted August 30, 2021, date of publication September 7, 2021, date of current version September 15, 2021.

Digital Object Identifier 10.1109/ACCESS.2021.3110873

LoRa IoT-Based Architecture for Advanced Metering Infrastructure in Residential Smart Grid

JOSÉ LUIS GALLARDO[1], MOHAMED A. AHMED[1,2], AND NICOLÁS JARA[1], (Member, IEEE)

[1]Department of Electronic Engineering, Universidad Técnica Federico Santa María, Valparaíso 2390123, Chile
[2]Department of Communications and Electronics, Higher Institute of Engineering and Technology–King Marriott, Alexandria 23713, Egypt

Corresponding authors: Mohamed A. Ahmed (mohamed.abdelhamid@usm.cl) and Nicolás Jara (nicolas.jara@usm.cl)

This work was supported by the Agencia Nacional de Investigación y Desarrollo (ANID), Proyecto Fondecyt de Iniciación en Investigación 2020, under Project 11200178.

ABSTRACT Internet of Things (IoT) technologies are opening new opportunities and services for different smart grid applications such as advanced meter infrastructures (AMI), distributed energy resources, and electric vehicles. Among these applications, AMIs represent the first step toward future smart grid implementation by enabling the reading and recording of electric power consumption on request or a schedule. In this study, the main focus is designing an IoT-based architecture to support AMIs' daily reporting and billing in a residential grid. First, the network modeling for AMI is discussed. Long range (LoRa) technology, as one of the promising candidates for long range low power wide area networks (LPWANs), has been studied and discussed. A comprehensive analysis of the LoRa-based architecture is given for a case study of an actual residential grid, Puerto Montt, Chile. The results are analyzed and discussed for packet delivery ratio, energy consumption, throughput, number of collisions, and frequency distribution.

INDEX TERMS Smart meters, Internet of Things, residential grid, LoRa.

I. INTRODUCTION

Nowadays, electric power utilities are moving towards grid modernization addressing many issues such as shortage of skilled workforce, aging assets, and regulation requirements for increasing awareness of environmental and emission concerns [1]. Under this scenario, the smart grid (SG) concept aims for a new electrical power grid, which replaces the traditional one-way communication grid by enabling two-way communication between customers and utilities. Furthermore, it enables the operation of different applications such as smart meters, distributed energy resources, real-time measurements, monitoring systems, and fast response using reliable communication and information exchange [2]. Advanced metering infrastructure (AMI) represents the first step towards smart grid as they provide the necessary infrastructure to support wide system measurement and visibility [3]. Automatic communication between customers and utilities [4], reduced tampering [5] and enabling customers to respond to their expectations to manage and generate their own electricity [6] are among the direct benefits of the smart grid infrastructure. However, with advances in wireless technologies, a knowledge gap in the analysis of the capability of recent technologies to support multiple applications of the AMI system is identified [7].

AMI brings many benefits to both utilities and customers. It provides bi-directional communication that enables the delivery of real-time consumption from households and production information and then disseminates such real-time information to utilities and customers [8]. The communication network supporting AMI can be divided into different sub-networks, such as utility-side network (UN), wide area networks (WANs), neighborhood area network (NANs), and home area networks (HANs). The UN concerns the utility domain, while WANs provide the physical medium to communicate between utilities and households on a large scale, which must meet the requirements of reliability and availability [9]. The NANs support data aggregation from groups of houses using data aggregation points (DAPs) or data concentrators (DCs) that collect the data sent from HANs. The HANs represent the internal home network at customer premises, where customers connect their appliances to the electrical grid, and their consumption is measured by a smart meter (SM). From this perspective, HANs are one of the core components of AMI, given their data generation capabilities (i.e., electric measurement). Therefore, its communication

The associate editor coordinating the review of this manuscript and approving it for publication was Bin Zhou.

This work is licensed under a Creative Commons Attribution 4.0 License. For more information, see https://creativecommons.org/licenses/by/4.0/

with utilities and reception of control and price signals are critical components of the AMI system.

NANs are crucial in deploying AMI networks because their traffic is related to SMs (i.e., periodic, delay-sensitive, and often fixed payload packets). Therefore, appropriate communication schemes must be considered in the design of NAN [8]. Considering the economic constraints and the flexibility in AMI installation when deployments are performed in different environments, wired schemes are not feasible owing to many significant drawbacks [10]; however, their high data rates, reliability, and robust interference mechanisms must be considered. On the other hand, wireless-based solutions are good candidates for use in AMI deployments owing to their low cost, scalability, and connectivity in inaccessible areas [2].

NANs are expected to serve a significant number of applications, in addition to SM data collection, such as outage detection, demand response, electric vehicle charging, and security distribution [11]. Among the different traffic types that can be found in AMI networks are: scheduled meter reading, on-demand meter reading, time-of-use (TOU) usage, firmware updates, and outage and restore management (ORM) [4]. Each type of traffic has a specific behavior [11], which can be summarized as follows: given the nature of applications, upstream traffic volume will be higher than downstream; traffic per region will vary and so the requirements (i.e., traffic profile will not be the same); all links must be operating and have available resources when smart meters send measurement data which is a critical and resource-demanding task of the network; and alert overhead (additional data rate requirements are added when networks operate under emergencies).

When planning the communication network of AMI, a vital consideration is that AMI devices communicate in frequency bands that can be easily monitored to protect the devices from being jammed or compromised [12], especially at NAN premises. The use of encrypted communication, which may add overhead, can provide an extra layer of defense for AMI communication, achieving integrity, availability, and confidentiality of data. In order to minimize delay, proper scheduling of data transmission and gateway location are among the problems that need to be considered in the design of an AMI network [11].

Low power wide area network (LPWAN) is a technology mainly targeted for M2M and IoT networks, in which devices can last up to 5-10 years by relying on batteries [13]. With the introduction of these technologies, new services can be expected to support data collection [14]. Various organizations in the industry, academia, and government have begun implementing such solutions to collect numerous types of data using sensor devices [14].

It is important to note that the AMI networks can be considered operational technology (OT) networks and not as proper information technology (IT) networks. The reason for this is due to the natural difference between these domains: IT includes traditional computing, storage, and telecommunication systems, while OT includes technologies that run real-time processes such as electricity distribution, manufacturing plants, and transportation systems [15]. Smart meters are the core of OT and part of the electricity distribution network, but the meter data management system (MDMS) and back-office (not visible to customers) functions are IT applications. Given the importance of both domains, a convergence has been increasing in many industries.

This work aims to fill the research gap related to the feasibility of LoRa technology in supporting AMI in a real suburban neighborhood area network. First, we proposed an IoT-based architecture for AMI, consisting of three layers: the perception layer, communication network layer, and application layer. Details about network modeling and simulation for the communication network layer were considered using the FLoRa simulator. An actual case study for a residential grid in Puerto Montt, Chile, is considered. The results are analyzed and discussed in terms of packet delivery ratio, energy consumption, throughput, and number of collisions.

II. RELATED WORK

The main components of the AMI network are smart meters, data aggregation points (DAP), and meter data management systems (MDMS). Several studies have been done (simulation and implementation) to prove that emerging technologies can satisfy the needs and demands of AMI networks in terms of scalability, data rates, energy-aware schemes, collision avoidance schemes, and terrain constraints.

Concerning network design, specific cases and constraints were provided for the network domain. The authors in Ref. [16] investigated the capacity analysis of a wireless backhaul for smart meters in a smart grid. Uplink traffic from smart meters to utilities is more interesting in terms of network capacity, as these have more data to deliver than the opposite downlink communication. The importance of this process is advised in [1], where the communication network infrastructure must be built in such a way that supports long-term operation and business requirements. Such a design should support future network extensions such as expected future applications and technology development and trends.

Regarding communication network design, the authors in [4] presented two main scenarios of AMI operation: regular operation, also known as scheduled meter reading, when all customers are receiving the corresponding electric power; and the outage and restoration management (ORM) scenario, when there is an electric outage affecting a group of customers and more control messages flowing on the AMI network. According to Ref. [11], SMs can support a wide range of data collection frequencies that can be configured remotely. Residential premises can be polled every 5 to 60 minutes, while industrial or commercial premises can be collected in seconds. This data collection frequency, along with their traffic volume, will vary for every utility depending on their metering systems and specific needs for

TABLE 1. Comparison among previous work of LoRa networks for IoT implementations in AMI.

Reference	Work Type	Area of Application	Used Neighborhood	Comment
[2]	Theorical - Survey	SM-DAP-Utility	Generic	Authors presented the state-of-the-art for smart grid technology and described the devices involved, architecture for AMI deployments, communication schemes, and data traffic requirements.
[4]	Simulation	SM-DAP	Urban - Real Case Study	Network and capacity planning for AMI deployments in an urban environment using a Narrow-band IoT scheme. The results are presented in terms of the SNR, RSSI, and coverage.
[5]	Simulation	SM-DAP	City of Medan, Indonesia	Good theorical approach using Medan as case study, lacks of simulation or performance evaluation of proposed solution.
[7]	Simulation	SM-DAP-Utility	Real case study	Peformance analysis of different communication schemes for AMI networks applied in a real-world scenario, in terms of throughput and latency.
[8]	Simulation	SM-DAP-Utility	Laboratory Setup	Experimental demonstration of the AMI network communication using the NS-3 simulator and different backhaul technologies to connect SM to utility, such as LTE, WiMAX, Wi-Fi and CoAP.
[11]	Simulation - Network planning	SM-DAP	Generic	Proposed network planning method to optimally allocate a gateway to the AMI networks. Data traffic types, delivery ratio, delay, and collection time were the main parameters of the study.
[13]	Implementation	IoT application in urban scenario	University campus	Implementation of LoRa end-devices communicating weather information, provides feasibility study for LoS and NLoS.
[14]	Implementation	IoT application using LoRa in urban scenario	University campus	Implementation of a case study for LoRa technology to evaluate the scalability of LoRa networks without carrier sense.
[15]	Implementation	Service and rescue operations	Harsh environments	Implementation of LoRa technology in harsh environments and proves the usability of LoRa for critical operations
[19]	Simulation	SM-DAP	Generic	Simulation regarding different packet size, transmission frequency and traffic types are carried out, analyzing transmission times and how an AMI network behaves by changing these parameters.
[24]	Implementation	IoT application using LoRa in agricultural premises	Rural premises	Implementation of LoRa to provide smart fenses for agricultural applications, proving that LoRa is capable of delivering high-quality links; however vegetation has a considerable impact on link quality
[25]	Theoretical	General, all-in-one	General Study	Theoretical study of LoRa links, applying obtained results for possible use cases in terms of reliability, scalability and performance.
[29]	Architecture	SM-DAP-Utility	Generic	Layered architecture proposed to support smart grid traffic, considering the power, access, service, and application layers. Power demand and time were the main parameters of the study.
[31]	Architecture	SM-DAP-Utility	Generic	Application of IoT network communication paradigm in smart grid deployments, defined by considering several layers: collection, communication and processing.
[32]	Implementation	SM-DAP	Laboratory Setup	HAN-NAN communication using ZigBee communication scheme, using a laboratory implementation and a single coordinator node.
[34]	Implementation	SM-DAP	University campus	Narrow-band IoT performance evaluation, considering university campus implementation. The results were analyzed in terms of coverage, reliability, latency, battery life, and security.
[46]	Simulation	SM-DAP-Utility	Generic	Feasibility study of the LoRa scheme for AMI deployment, in terms of delivery ratio, energy consumption, number of nodes and operational parameters of LoRa.
[47]	Architecture - Network Planning	SM-DAP	Real case study - Urban, suburban and rural	Network planning based on a clustering algorithm, optimal deployment topology generation based on the SM and DAP locations. The node distribution, distance, coverage density, and execution times were evaluated.
Present Work	Simulation	SM-DAP-Utility	Real case study - suburban	Performance analysis of LoRa communication used on NAN premises, taking as input topology the model developed in [47] applied in a real suburban neighborhood as a case study

implementation [3]. In Ref. [17], the authors defined three types of AMI traffic: periodic keep-alive (packets every 1 min), periodic response/request (packets every 240 min), and aperiodic alarm-based (on demand). As several utilities may exist, data traffic from smart meters will have different packet sizes according to the requirements [11]. In general, SM traffic presents the following patterns [18]: small packet size, large amount of packets in the network and interval timing requests. For small applications, such as remote meter reading, a small packet is sufficient (i.e., 20-500 bytes), but when applications scale in complexity, the packet size may increase as well (up to 40000 bytes) [19]. On the other hand, industrial appliances may require more control, monitoring, and updates, as they are more prone to load variation in comparison to residential zones [20].

For network planning, the authors of Ref. [5] presented a framework for network and capacity planning that takes into consideration parameters such as link budget (Okumura-Hata model), number of gateways, area/surface to cover (in numbers), and cell size. Given that the scope of application is theoretically applied to a case study in a specific city, the work did not consider a simulation or performance evaluation of the proposed solution. To design a communication network for AMI, the capacity of the backhaul network and the number of smart meters covered by base stations determine the expected delay of communication [20].

Regarding protocol usage, in [16], CoAP is chosen as the primary application protocol given the traffic type that will flow through the AMI network: control commands, load profile generation, and log data from SMs. As these packets are small, communication must be fluid using specialized protocols for these tasks. The authors in [1] stated that UDP over IP is preferred, given the data traffic volume and quantity that AMI networks will operate. However, when reliability is a critical constraint, TCP-based communication must be employed or implement reliability mechanisms under the application layer. In [20], when comparing TCP and UDP for M2M communication for SM IoT-based scenario, concerning delays, UDP achieved better results.

Considering IoT architectures, and as AMI networks are a particular case, the AMI network must achieve two main goals [5]: efficient communication (i.e., massive connectivity) and defense against environmental conditions. The capabilities of LoRa wireless scheme, shown in Ref. [21], are demonstrated with an implementation of an end-to-end temperature measurement system. The authors in Ref. [22] presented time-performance indicators for LoRa technology when applied to distributed systems in IoT, providing insights and proving that for smart metering, smart building, and process industry fields is a promising scheme.

The actual implementations of AMI have been considered in different case studies. The authors in Ref. [3] showed an already implemented AMI network using a 900 MHz RF-mesh network alongside cellular networks, polling data at different rates. In another experiment, but with security purposes, the authors in Ref. [12] used the IEEE 802.15.4 radio technology to test AMI technology. 900 MHz RF-mesh networks were the most popular in the United States. Details of the real AMI deployments of the SM networks are given in Ref. [7].

In the particular case of LoRa technology, several aspects have been covered in different case studies to prove that this scheme can meet the minimum communication requirements for AMI networks. The authors in Ref. [22] compared LoRa technology with wireless local area networks (WLANs) and RF devices for service and rescue operations in extreme environments. Evaluations were performed in terms of battery consumption, range, and link robustness to shadowing. In conclusion, LoRa technology could achieve a high delivery ratio in adverse conditions (i.e., snow). A line-of-sight (LoS) and non-line-of-sight (NLoS) study based on the received strength signal indicator (RSSI) and delay was carried out in Ref. [13], where the authors indicated that LoRa technology could be efficiently used for industrial IoT applications. However, the study has not pointed to SM or AMI traffic, nor how scalability issues can be addressed on these networks when operating with LoRa. In Ref. [14], the authors carried out a performance evaluation of an actual implementation of LoRa technology for IoT architecture. In terms of collisions, they state that these networks do suffer from collisions if carrier sense mechanisms are not enabled and, if the number of nodes in the network increases, a mechanism is needed to ensure reliability against communication issues and proper network scaling.

On the other hand, LoRa technology can be deployed at agricultural premises, as given in Ref. [24], depending on the obstacles presented in the LoS of links, which has a direct effect on the signal-to-noise ratio (SNR) value; nonetheless, LoRa performs well, making it feasible for rural premises. Finally, a theoretical analysis of LoRa links is presented in Ref. [25], where the authors showed that a single LoRa cell could handle up to millions of nodes. However, they stated that devices with critical constraints of uplink traffic must be placed near the gateway, and delays are of concern when devices are located far away from the gateway (i.e., when networks start to scale to thousands or million devices). The idea of LoRa networks is to communicate directly with nodes, removing the need to reconstruct and maintain a complex hop network [26].

The effect of multiple gateways is discussed in Ref. [27]. When using a single gateway configuration, the duty cycle limitations restrict the convergence time and ADR functionality. However, when deploying multi-gateway networks, and as these are deployed in the field, nearby nodes can communicate with their nearest gateway, reducing convergence times, increasing data rates, and dealing with higher traffic loads. This situation does not add more complexity, as gateways act as relays for the network server and are the primary method of increasing scalability. In addition, it contributes to improving the network performance by the balancing load between gateways [27].

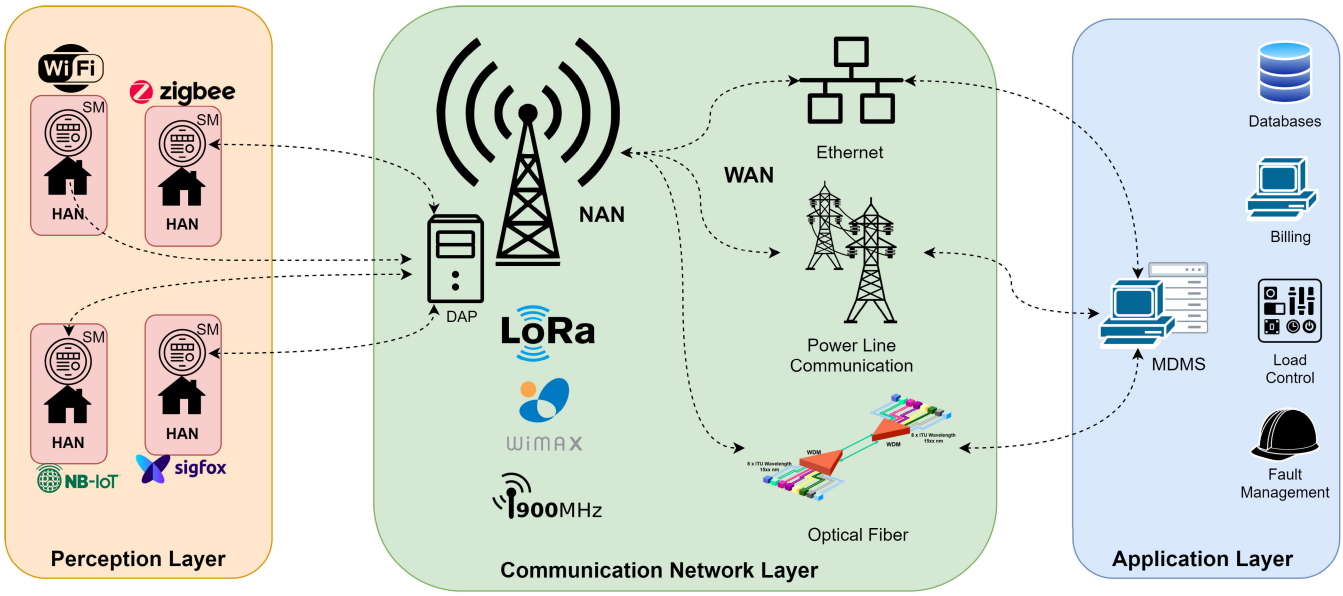

FIGURE 1. IoT based architecture for AMI in residential grid.

This work studies the feasibility of LoRa technology for supporting an AMI network. The main contributions are: (1) Proposing an IoT-based architecture for AMI, which consists of three layers: perception layer, communication network layer, and application layer; (2) Development of a ready-to-deploy topology given by the output of a network planning process; (3) Study the feasibility of LoRa technology as a promising candidate for supporting AMI network deployment; (4) Performance evaluation of the communication network layer for a real case study of a residential grid in Puerto Montt, Chile. The results were evaluated for data delivery ratio, energy consumption, throughput, collisions, and frequency distribution.

III. IoT-BASED ARCHITECTURE FOR AMI

The advanced metering infrastructure (AMI) consists of four different network domains: home area network (HAN), neighborhood area network (NAN), wide area network (WAN), and utility network (UN). The HAN is related to the communication between appliances and the smart meter (SM). The NAN is related to the communication between smart meters and a concentrator device called data aggregation point (DAP), which acts as a gateway to gather data from houses. The WAN is related to the communication channel between DAPs and the utility network, which must deliver the data generated by SMs to utility premises. The UN is related to all data tasks that utilities are in charge of, such as billing systems, demand response (DR) programs, control, and grid administration.

On the other hand, Internet of Things (IoT) technologies enable physical objects to see, hear, think and perform jobs by having them "talking" together in order to share information, and coordinate decisions [28]. IoT technologies will transform static devices into smart devices by exploiting their underlying technologies, such as ubiquitous and pervasive computing, embedded devices, and communication technologies. In terms of dimensions, smart objects with their tasks generate specific applications and services that can transform them into different domains. The main benefit of the use of IoT in smart grids is the contribution to the quality of life and growth of the world's economy. As this will open a new world of benefits, applications must grow proportionally to match the required needs of industry and customers; and devices must also be developed to fit customer needs in terms of availability anywhere and anytime.

In order to merge both already described worlds, certain characteristics must be accomplished: flexible layered architecture, given the heterogeneity of possible connected objects and critical tasks that they must complete. To meet these requirements, several authors have proposed different architectures as a general topic to approach this task [1], [28]– [31]. Figure 1 shows the IoT-based architecture for AMI in a residential grid.

A. PERCEPTION LAYER

The perception layer consists of sensor nodes and measuring devices. Here, the physical sensor level covers data collection and processing. Different types of sensor nodes and measuring devices such as meter reading, location querying, temperature reading, motion sensors and humidity can be found. Several devices can also be found at the home/building level, such as home appliances, home energy management systems (HEMS) and SMs. In this work, we consider smart meters in this layer as fixed points where smart meters send

their data to utility premises, forwarding it to the following layers.

B. COMMUNICATION NETWORK LAYER

The communication network layer is in charge of communicating among end devices (perception layer) with MDMS servers and vice versa. The first task of this layer is to enable data transfer under secure channels of measurements using different transmission media. The second function is the storage function, which can be met using middleware software that communicates with the storage servers and the different devices that can be found. WAN and NAN are the core networks in this regard, and must be designed to meet different requirements for reliability and availability for data links. In this domain, several wired/wireless communication schemes can be found, such as optical fiber, WiMAX [10], ZigBee [32], LoRa [21], [33], and NB-IoT [34].

C. APPLICATION LAYER

The application layer is in charge of all the tasks related to data processing, display, and disposition of data to customers and utilities for the different applications that are intended. For customers, smart services and remote management must meet different requirements. For utilities, business-side tasks include business model applications, graphs, flowcharts, and big data analysis for the perceived data from the perception layer. Under this domain, the following applications may coexist: user dashboard and measurement display, meter data management system (MDMS), and billing systems. An important constraint for this layer is that, as both customer and utility data will be stored and operated together, both must share a common protocol or communication interface to speak with other systems. An example could be using utility on-premise servers to store customer and company data, along with cloud storage as a backup method.

IV. LoRa TECHNOLOGY FOR AMI COMMUNICATION

LoRa is known as the PHY layer of communication defined by the Semtech Corporation [35]. It operates under an ALOHA transmission scheme and uses the chirp spread spectrum (CSS) as a modulation technique, and usable channels are quasi-orthogonal [36]. The most important features of LoRa technology are small data transmission, low energy consumption, and a high communication range, enabling long-distance communication. Several parameters are configurable for this layer, as follows:

1) Transmission power (TP): the transmitted power by LoRa devices ranges from -4 dBm to 20 dBm at 1 dB steps.
2) Carrier frequency (CF): center frequency of operation ranging from 860 MHz to 1020 MHz. This value depends on the region in which LoRa devices operate (e.g., America, Europe).
3) Bandwidth (BW): frequency range of the CSS represents the chip modulation rate for LoRa. Three possible values can be selected: 125, 250, and 500 kHz. Higher bandwidths give higher data rates but lower sensitivity, and vice versa.
4) Spreading factor (SF): ratio between the data symbol and chirp rates which is an exponential factor. A higher SF means a higher SNR (i.e., sensitivity and range) and a lower data rate, and vice versa. Values range from 7, 8, 9, 10, 11, and 12. When increasing sequentially in SF, the transmission power is halved while the transmission time and energy are doubled.
5) Code rate (CR): The forward error correction (FEC) rate affects the time-on-air packet transmission. A high code rate translates into more possibilities for detecting and repair data errors at the bit level. Values range from 4/5, 4/6, 4/7, and 4/8. Radios with different CRs can only operate if they use an explicit header (the payload CR is included in the header of the packet).

In [5], LoRa data rates vary between 0.3 and 27 kbps for each channel in order to save the battery, which the SF commands in use on devices. It uses chirp spread spectrum (CSS) modulation as a PHY layer. Under this scheme, symbols are encoded into chirps, which are signals whose instantaneous frequency sweeps linearly through the bandwidth [37] according to the chosen spreading factor and particular initial value. One symbol carries SF bits; then a CSS signal carries $M = 2^{SF}$ different symbols, each one of them distinguished by an individual chirp with different starting frequencies. Device communication with different SFs can be possible because frequencies are quasi-orthogonal to each other [38] and network separation between SFs is possible. The transmission time on air is greatly affected by the correct decision of the parameters mentioned above and payload size. For example, a packet with 20 bytes can vary from 9ms to 2s. Hence, this parameter has a tremendous impact on the scalability of LoRa deployments.

Regarding physical access to the spectrum, limitations depend on the regulations of each country. These limitations can affect the performance and scalability of LoRa deployments due to the excessive use of available bands by other applications not related to LoRa. it is important to note that technical or operational requirements are not an issue for good LoRa operations. Concerning packet size, as several studies have used their packet size according to their needs, there is no standard referring to packet size relative to every application's domain. Packet size includes headers and payloads, each of them with its corresponding CRC bits. However, the maximum payload size for a LoRa frame is 256 bytes [39].

LoRaWAN is the MAC layer that operates over LoRa networks and is defined by the LoRa Alliance. The devices under this scheme operate using a star-of-stars topology [35]. As stated in Ref. [13], there exist three classes of communication for LoRaWAN devices, all of them are bidirectional:

1) Class A: uplink transmissions followed by downlink and devices have the lower power consumption. Smart meters are classified in this category.

2) Class B: scheduled reception at predefined time slots (i.e., beacon frames at predetermined intervals).
3) Class C: devices are always in reception mode upon transmission, making control data receivable at any time. These types of devices are found in industrialized domains, where maximum control is required at any time, and energy constraints are not a problem.

The LoRaWAN has a critical component named adaptive data rate (ADR), which controls the performance of the LoRa network by modifying the data rate parameter (i.e., SF) based on current wireless channel conditions. In the initial conditions, there exists a convergence time that helps the network to reach its optimal operation [40]. With the correct selection of transmission parameters of end-devices, these can operate in an energy-efficient manner (i.e., reducing their overall energy consumption), increasing the overall packet delivery ratio, and, therefore, make networks scalable. For these reasons, using this component when LoRa networks operate is optional, but highly recommended.

Given the importance of this mechanism, explanations of its operation must be provided. The mechanisms operate on two sides: end-device side (end nodes) and network server-side:

1) End-device side: the ADR is defined in the LoRaWAN protocol specification. If the node does not receive an ACK packet when requested, the data rate decreases (i.e., SF increases, thus increasing the communication range). For each uplink frame sent without a downlink response frame, this process is repeated. The end-devices algorithm commands the time employed to decrease data rates. The flow chart explaining how this mechanism operates is shown in Figure 2.
2) Network server-side: there is no official definition of ADR, but Semtech Corporation recommends the following implementation. The network server (or gateway) records the highest SNR value for each incoming packet and, if the device associated with the device does not use the fastest data rate and the lowest transmission power, it calculates the expected most suitable data rate for the device. Then, this new value is assigned to the end-device according to its current data rate and received SNR values, and it is transmitted to end-devices via downlink frames. This algorithm increases the data rate (i.e., decreases the SF), and the network server algorithm commands the time employed to increase data rates. The flow chart explaining how this mechanism operates is shown in Figure 3.

Several benefits can be found when operating LoRa networks with ADR mechanism. A single gateway can handle many end devices and enables nodes to reactivate their links to the gateway when the connection is lost by gradually increasing the data rate. Given the intrinsic characteristics of the CSS modulation scheme, LoRa links are robust against multipath fading and interference phenomena. This situation is explained by the use of frequency hopping at each

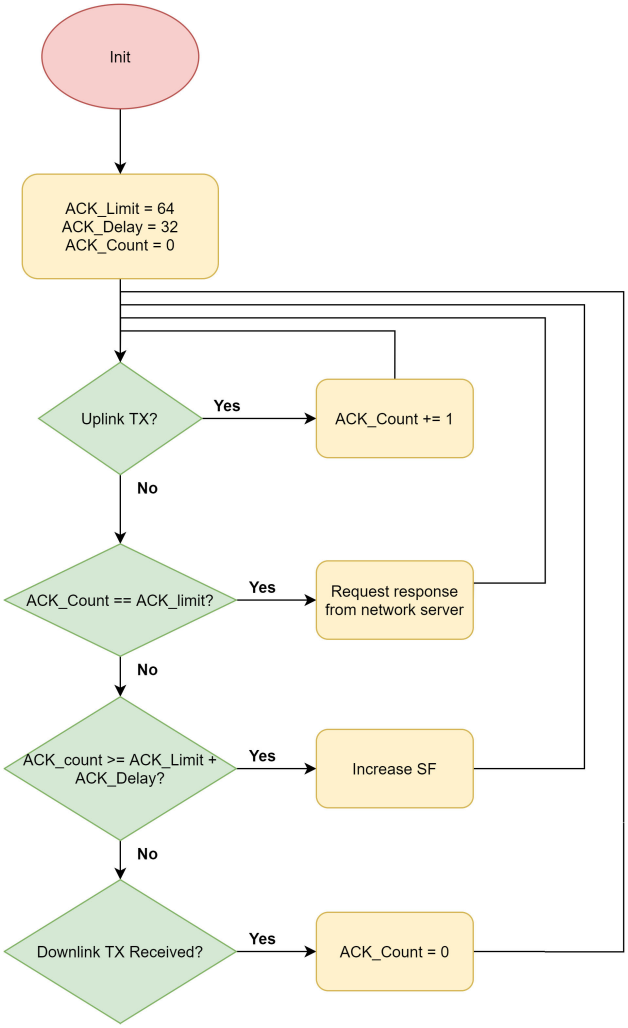

FIGURE 2. Flowchart of ADR mechanism at node side.

transmission (i.e., each device operates at different spreading factors), as this mechanism is used to mitigate them [41]; however, certain combinations are more convenient when deploying networks that require long-distance communications [42]. In addition, as signals may be reflected or refracted on surfaces, and as CSS signals are spread over the entire bandwidth, signals with constructive or destructive interference will be collected, owing to the energy distribution in the entire bandwidth. Finally, given the orthogonal nature of the spreading factors, this allows for the proper reception of signals simultaneously [43].

However, a possible drawback of ADR is the nature of IoT communication. It must be performed when is strictly necessary. Hence, when sending acknowledgements to end-devices, these messages may not arrive at the destination given the restricted duty cycle constraints of operation [45], and may arrive when it is too late for end-devices (lost communication). Also, as several devices may join the network, convergence times may increase as the nodes are redistributed (in frequencies) to support an optimal operation.

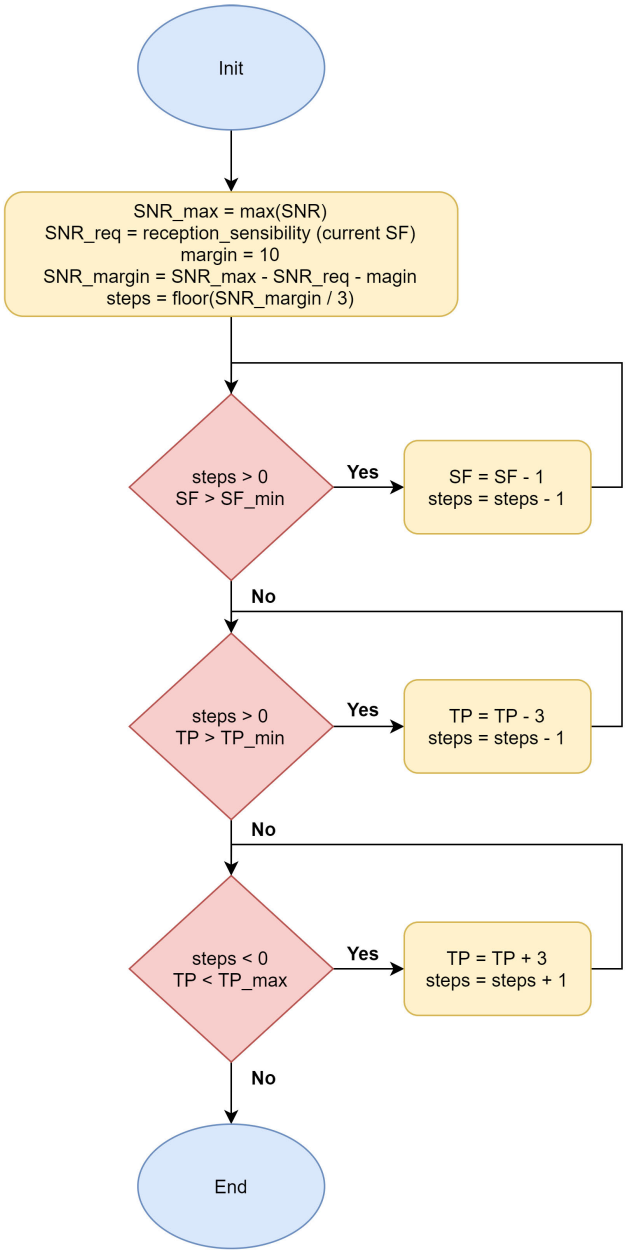

FIGURE 3. Flowchart of ADR mechanism at server side.

The importance of operating with an ADR mechanism was advised by [26], where the authors showed that LoRa networks do not scale well when operated under static settings, and a single gateway for an extensive LPWAN network is not sufficient. In AMI networks, all changes in channel conditions are handled and performed by the gateway. In this case, the DAP must handle hundreds to thousands of devices.

V. SIMULATION SETUP

Regarding the simulation setup, certain initial conditions must be considered when deploying the AMI network in this case study:

1) Initial data rates: each device starts with a randomly assigned data rate (or spreading factor). The convergence time will depend on the number of nodes and the initial SFs. The random choice of SF is justified as follows: if every node has the highest SF, the end-device ADR mechanism will operate on every node, making convergence times higher and, possibly, generating a high number of collisions. On the other hand, all devices with lower SF will converge at a higher rate with respect to end-device algorithm as the gateway can manipulate all nodes considering any set of possibilities.
2) New nodes join the network: if the network has a specific order, new nodes may interfere with the current order, making a new reorganization process as new nodes may not be using the optimal SF.
3) Final data rates: the final distribution of SFs will vary depending on the distance between the nodes and the gateway and the number of nodes in the network. It is possible that every node can have the same SF if there are no numerous collisions.
4) Arbitrary implementations of ADR in LoRaWAN: as there is no standard for deploying or implementing the ADR mechanism at the network server-side [44], issues can arise: if end-devices do not transmit uplink frames, the possibility of not receiving downlink ACK or control frames is high, leading to keep the data rate without any changes. Hence, energy limitations and scalability issues may occur. To address this, we consider the implementation of FLoRa for the ADR mechanism [46]. LoRa Alliance defines the ADR mechanism operating at end-devices (i.e., increase only SF), while the ADR mechanism operates at network server-side estimate link quality using SNR values and changing TP decreasing SF if necessary.

Regarding LoRa PHY modeling, FLoRa uses the log-distance path loss model with shadowing, which calculates the path loss based on the distance between the transmitter and receiver, as given in Equation 1.

$$\begin{aligned} PL(d) &= \overline{PL}(d_0) + 10n \cdot log(\frac{d}{d_0}) + X_\sigma \\ &= P_{TX} - P_{RX} \end{aligned} \tag{1}$$

Re-arranging the terms, we obtain the reception power at the receiver in dBm, as given in Equation 2.

$$P_{RX}(d) = P_{TX} - \overline{PL}(d_0) - 10n \cdot log(\frac{d}{d_0}) - X_\sigma \tag{2}$$

where P_{RX} is the reception power at the receiver, P_{TX} is the transmission power of the end-devices, $\overline{PL}(d_0)$ is the mean path loss for distance d_0, n is the path loss exponent, d is the distance from the gateway and end-device, d_0 is the path length, and X_σ is a zero-mean Gaussian distributed random variable with standard deviation σ modeling the shadow fading or slow fading of the links.

It should be noted that the range can only be changed by changing the transmission power. Other PHY parameters (i.e., SF, CR, and BW) did not have any influence. However, on the receiver side, the communication range is limited by the sensitivity threshold S_{RX}, which is influenced by LoRa parameters such as SF and BW. Most implementations of propagation models use the log-distance path loss model, which is commonly used for studying deployment in densely populated areas. The simulation parameters are presented in Table 2.

TABLE 2. Simulation parameters.

Parameters	
Carrier Frequency	915 MHz
Bandwidth	125 kHz
Coding Rate	4/8
Spreading Factor	7 up to 12
Transmission Power	2 dBm up to 14 dBm
Path Loss (σ)	3.57 dB
Path Loss Distance (d_0)	40m
$\overline{PL(d_0)}$	127.41 dB
Path Loss Exponent (n)	2
Number of Gateways	1
Number of Nodes	34, 68, 102, 136, 170
Payload Size (end-devices)	20 Bytes
Payload Size (control)	15 Bytes
Packets sent	{12, 24, 48, 96} per day

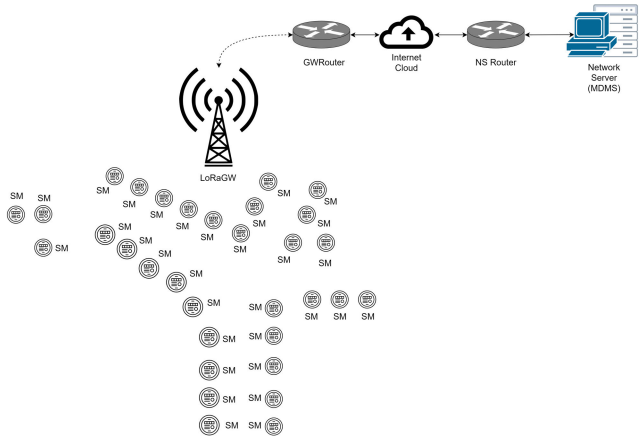

FIGURE 4. FLoRa implementation topology.

VI. IMPLEMENTATION RESULTS

In this section, we present the data used to test the AMI network's performance using LoRa PHY and LoRaWAN MAC technologies alongside their respective metrics. The primary study parameters are the delivery ratio (DR), energy consumption (EC), throughput, number of collisions, and SF distribution. The simulation was performed on a 3 GHz 9th generation Intel Core i5 CPU with multi-threading, 8GB of RAM, and running Ubuntu 20.04. The simulation tool used is the FLoRa simulator developed by the authors of Ref. [46], based on the network framework OMNeT++.

A. NEIGHBORHOOD AREA NETWORK

A real neighborhood was employed to evaluate the performance of the AMI network. The suburban neighborhood is located in Puerto Montt, Chile. This case was chosen because the suburban study for the NAN is aligned with the work presented in [47] for planning the AMI network. Smart meters are modeled by their (longitude, latitude) coordinates obtained using Google Maps and modeled on an X-Y axis using imaging software to obtain a plane representation of the ground. This area is shown in Figure 5.

FIGURE 5. Suburban area - Puerto Montt, Chile.

We evaluated the performance of the AMI network by performing a total 12-day simulation of the network, from which we took the average of 30 runs or executions of the same scenario to obtain good comparison samples (owing to different random seeds and network behavior). Every simulation scenario was performed by increasing the number of nodes from 34 to 170, in steps of 34 nodes, to view how the network behaves. Given the flexibility in LoRa networks to operate with or without the ADR scheme, the following sections present the network behavior in the suburban neighborhood considering both scenarios, and a comparison between both schemes is presented. Finally, to study the message frequency in AMI networks, we considered four communication schemes: sending packets every 15, 30, 60, and 120 min.

B. CONVERGENCE TIME

This section presents the results from the simulation scenario regarding convergence time.

As presented in [40], the LoRaWAN MAC layer has an optional ADR mechanism that, if enabled, helps to recognize the network by changing the operation frequency of end-devices and transmission power to take advantage of the frequency ranges available in LoRa. As more packets flow in the network, the network server can have more data to

consider and make better decisions. This behavior is shown in Figure 6. We can observe that, when increasing the communication time, certain metrics start to converge. In this case, regarding delivery ratio, ADR-enabled behavior tends to stabilize after 12 days of operation, as variations of this metric are less abrupt. In the case of ADR-disabled, as there is no change in network operation, metrics can be considered the same during this period.

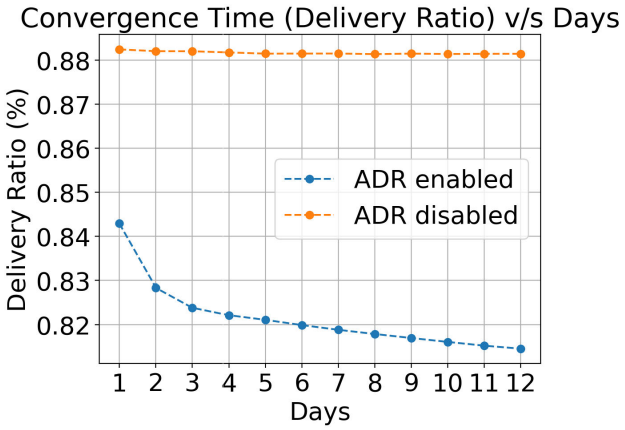

FIGURE 6. Convergence time.

Given this observation, we chose to simulate every scenario for a total period of 12 days, as storage limitations started to arise when storing per node and gateway metrics. Nonetheless, given the behavior of the curves, we conclude that if networks can operate for extended periods of time, the metrics will tend to converge to a specific value.

C. DELIVERY RATIO

This section presents the results from the simulation regarding the delivery ratio. The delivery ratio for LoRa networks is defined as the ratio between the number of messages correctly received by the network server and the total number of packets sent by every node, which gives a number between 0 and 1. If this rate is close to 1, the network can be considered with an ideal behavior, whereas a rate close to 0 means that every transmitted packet may not reach the destination. The results are shown in Figure 7.a and 7.b.

For a small number of nodes, LoRa networks with ADR-disabled achieve a better delivery ratio than those with ADR-enabled. This situation can be explained in the following context: a small number of nodes implies a less saturated spectrum and fewer possible collisions. Under these circumstances, network ordering can be optional when deploying these networks in small areas.

While increasing the number of nodes, the communication with ADR disabled tends to be more unstable than ADR enabled, as this value decreases dramatically from 0.99 to 0.88 in the case of 170 nodes. In contrast, for ADR-enabled networks, the value of the delivery ratio decreases at a lower rate which means that the network still achieves a steady state. The maximum decrease is 0.03 and 0.01 when transmitting 12 and 96 packets per day, respectively.

When varying the transmission frequency, all curves show a standard behavior corresponding to their frequency: more messages imply a lower delivery ratio, as more nodes are transmitting simultaneously and occupying the same channel. When the ADR is disabled, this translates into a more rapid decay value behavior, changing the value even for an 11% for the worst-case scenario (96 packets per day). However, when ADR is enabled, there is a slight increase in the delivery ratio value, which can be explained by more frequent changes in SF and transmission power in end-devices and, therefore, increases the overall network behavior for the same scenario (96 packets per day) when the node number increases.

From the results given, we can conclude that an ADR-enabled scheme is preferred for networks with a high density of nodes, as their performance does not decrease dramatically over time. Nonetheless, overall, the results for both schemes are over 85%, which is expected for a network with these characteristics. In general, ADR-disabled networks behave better than ADR-enabled networks with a small number of end devices; the delivery ratio decreases as the node number increases and transmission frequency for both modes.

D. ENERGY CONSUMPTION

This subsection presents the analysis of the energy consumption for end-devices obtained by the simulation for the suburban neighborhood, concerning the number of nodes and packet frequency. The plots are shown in Figures 8.a and 8.b. It is important to note that the energy consumption shown in the plots corresponds to the accumulated energy consumption of every node in the network in millijoule (mJ).

The ADR-disabled case shows that for every packet frequency, the energy consumption can be considered similar in every case for a small number of nodes (i.e., 34 and 68). A particular case is when the node number is doubled (from 34 to 68), where energy consumption increases from 166 to 195, translating into an overall increase of 14.87%, matching the big step in consumption. After that variation, the behavior tends to match what is expected. As more frequent communication between end-devices and the network server (i.e., utility domain) is done, this is translated into more energy usage from nodes, which is evident from curve behavior, reaching a top value of 225 mJ for the case of 15-min communication from 170 nodes.

On the other hand, when ADR-enabled networks are considered, the effect of transmission control is noticeable. When frequent transmissions occur in a network, this is the most energy-efficient scenario. This behavior can be explained by the activation of the ADR mechanism in the network, which takes place at least four times a day (96 packets per day). Compared to the case with ADR-disabled, the less frequent communication scheme has the worst energy consumption among the four cases. However,

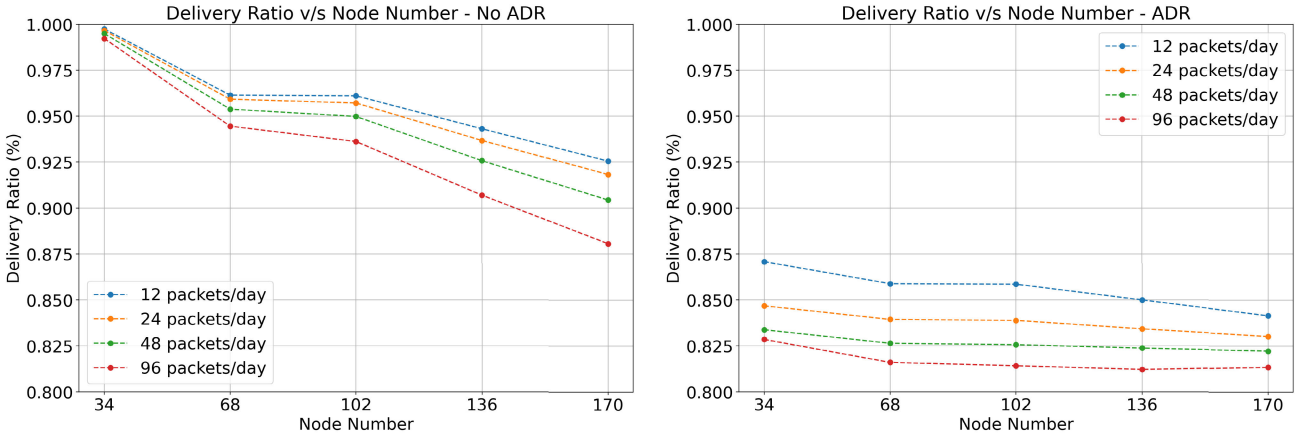

(a) ADR Disabled **(b)** ADR Enabled

FIGURE 7. Delivery ratio at network server.

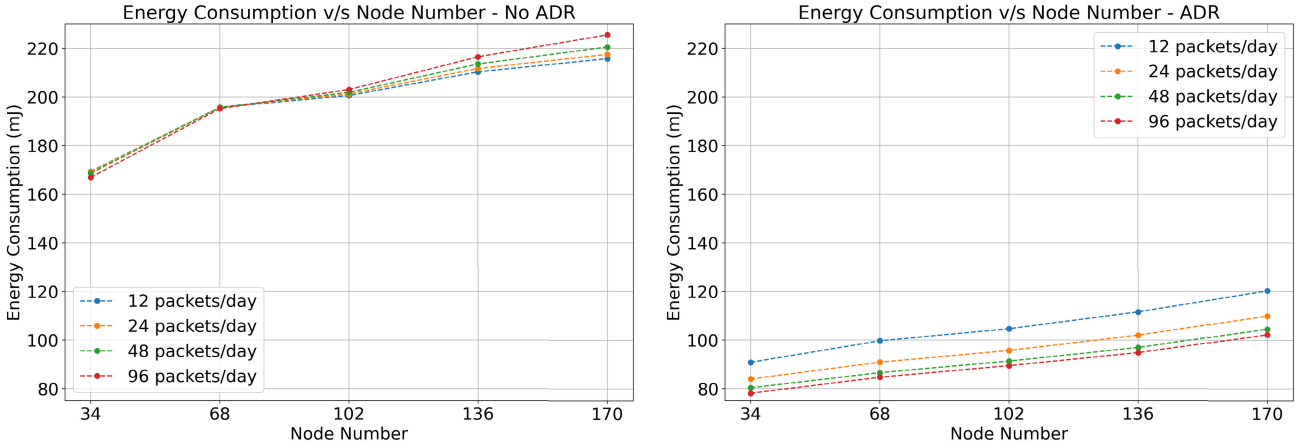

(a) ADR Disabled **(b)** ADR Enabled

FIGURE 8. Energy consumption for end nodes.

TABLE 3. Energy consumption for end nodes.

Energy Consumption (mJ)						
	12 packets per day			24 packets per day		
Node Number	No ADR	ADR	%	No ADR	ADR	%
34	169.33	90.82	46.37	169.12	83.96	50.35
68	195.67	99.66	49.07	195.74	90.85	53.59
102	200.56	104.63	47.83	201.22	95.72	52.43
136	210.31	111.59	46.94	211.69	101.99	51.82
170	215.74	120.17	44.3	217.47	109.93	49.45
	48 packets per day			96 packets per day		
Node Number	No ADR	ADR	%	No ADR	ADR	%
34	168.6	80.35	52.35	166.88	78.11	53.2
68	195.72	86.56	55.77	195.18	84.69	56.61
102	201.87	91.32	54.76	203.03	89.45	55.94
136	213.56	96.94	54.61	216.49	94.82	56.2
170	220.5	104.55	52.59	225.53	102.21	54.68

the four scenarios achieved better results compared with the ADR-disabled scenarios. Table 3 presents the results for both scenarios.

The results show that a substantial energy reduction of up to 56% can be achieved when deploying LoRa-based AMI networks, especially when frequent communication

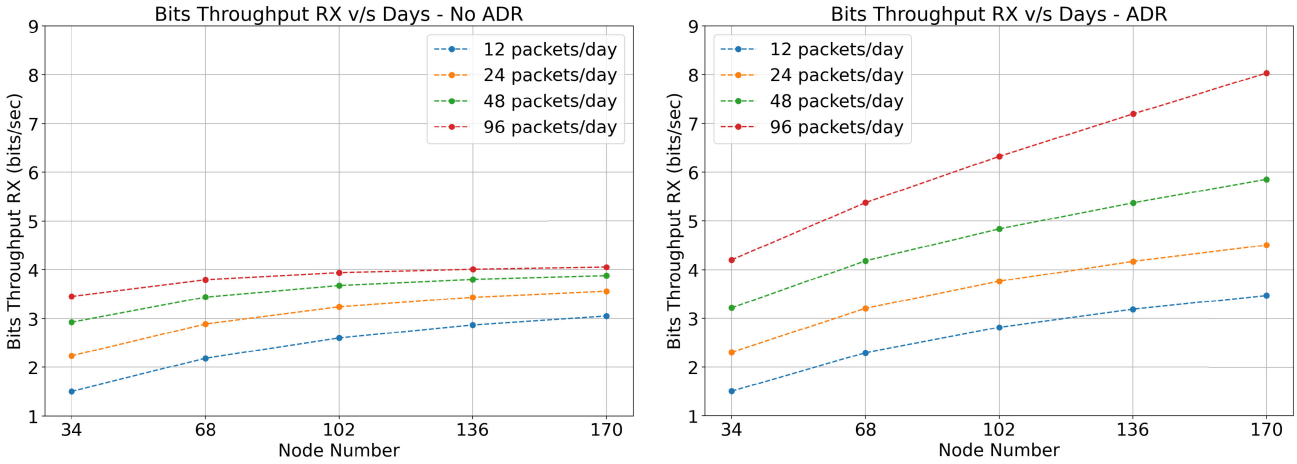

(a) ADR Disabled (b) ADR Enabled

FIGURE 9. Gateway reception throughput.

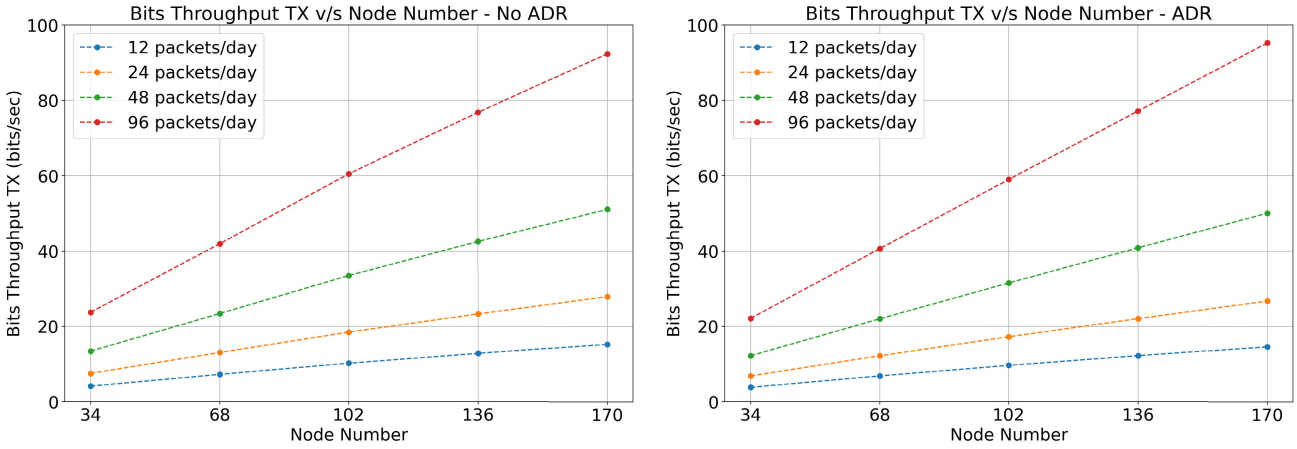

(a) ADR Disabled (b) ADR Enabled

FIGURE 10. Gateway transmission throughput.

from end-devices to the network server is present (96 packets per day). Energy reductions of up to 55%, 53%, and 49% were achieved when 48, 24, and 12 packets per day were transmitted, respectively.

Considering only this variable, the use of ADR in LoRa networks has a noticeable impact on energy consumption, making it a must-use feature for energy-constrained devices such as smart meters. It is important to note that, in countries that are still transitioning to apply new technologies such as LoRa, the entire electrical grid cannot be significantly changed, as it could affect millions of customers in different cities. Given this constraint, old meters will operate as SMs when a wireless battery-constrained device is attached to them. Under these circumstances, having a device configured with an optimal energy consumption pattern is very important to ensure the device's longevity and, therefore, for the AMI network.

E. THROUGHPUT

This section analyzes and comments on the throughput perceived by the gateway or DAP of the AMI network regarding uplink and downlink communication. The plots are shown in Figures 9.a and 9.b for reception throughput, and Figures 10.a and 10.b for transmission throughput.

The reception throughput corresponds to all the acknowledgment and control messages perceived by the gateway, which are sent to the end devices. With this information, and with ADR-enabled, a general improvement in speeds is perceived in every case (node number and packet frequency). As more data flows in this direction, we can infer that end devices tend to transmit only in their specified time windows with more network control on transmissions. Therefore, the network server can perceive more data from end-devices and send more acknowledgments, which explains the higher value of this metric. A significant improvement is perceived

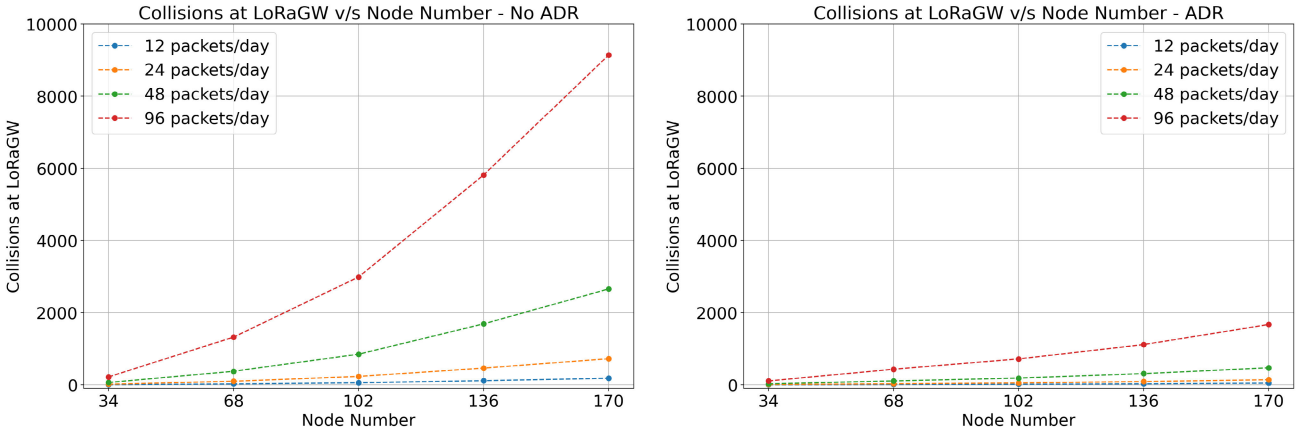

(a) ADR Disabled

(b) ADR Enabled

FIGURE 11. Collisions perceived by LoRa gateway.

when 96 packets per day are transmitted and when the node number is higher, which can also be related to the lower energy consumption. As more nodes have their transmission windows coordinated, there is less wasted energy when transmitting. In addition, the slight improvement in the delivery ratio can be attributed to this behavior.

On the other hand, networks operating with ADR-disabled perceive a convergence value in throughput, mainly when transmissions occur at a more frequent rate (48 and 96 packets per day). Owing to node number restrictions in our case study, we cannot conclude if there is a final convergence value. However, networks with lower packet transmission do not perceive this pattern. These results are similar to those of the ADR-enabled scenario.

As a result, the general perspective is that networks with a higher number of nodes can benefit from the ADR mechanism, as they can achieve higher reception throughput due to the spectrum order and reallocation of nodes (spreading factor changes). However, when networks have a lower number of nodes and their packet transmission frequency is not critical or of high importance, the ADR mechanism can be considered optional because the performances of both scenarios are very similar.

The transmission throughput corresponds to all the data flow that the gateway perceives and is forwarded to the network server, which corresponds to the data packets transmitted by the end devices. As the results for both scenarios (ADR-enabled and ADR-disabled) are very similar, we can conclude that networks operating with or without these mechanisms transmit the same amount of data. However, the big difference among them is how end devices transmit their data. As different SF changes occur with ADR-enabled, a better energy usage is achieved, and more acknowledgements and control messages flow from the network server to the end-devices.

The conclusion from this perspective is that it does not matter if the ADR mechanism is enabled or not; the data will be sent equally in either case. However, the internal order of node frequencies will make a big difference when utilities perceive the data from SMs when networks operate with a higher number of nodes, which is the case in many neighborhoods. If neighborhoods have a significant number of nodes, an ADR-enabled scheme will be preferred. However, if there is a small number of nodes, network operators can bypass this mechanism and operate without an ADR.

F. COLLISIONS

This section analyzes and comments on the number of perceived collisions concerning the gateway. The simulation results are presented in Fig. 11.a and 11.b. Table 4 provides detailed numerical insights for collision analysis.

The simulation results show that there is a noticeable reduction in collisions in the case of ADR-enabled networks. In the case of changing packet frequency or node number, the ADR-enabled networks show a better overall performance concerning collisions, with a reduction ranging from 4.67% to 0.85%, comparing ADR-disabled and ADR-enabled operations respectively, in their worst-case scenarios (96 packets per day and 170 nodes). When the packet frequency is low (12 packets per day) and the node number is high, this mechanism helps in providing better energy usage, a higher reception throughput, and fewer collisions. These benefits are achieved at the expense of a lower delivery ratio (compared to the scenario with ADR-disabled). Comparing ADR-disabled scenarios, improvements are seen by having less than 0.9% collisions, with respect to the total packets transmitted; consistent with the energy usage of the ADR-disabled scenarios and the continuous decrease in the delivery ratio value.

When the node number is low (i.e., 12 packets per day), for any value of the packet frequency, and comparing the total percentages of collisions, ADR-enabled networks present a general improvement ranging from 0.04-0.19%, which translates into better overall behavior. As node number continues to increase, as well as packet frequency, the percentage

TABLE 4. Collisions at LoRa gateway.

Collisions at LoRa Gateway.										
	12 packets per day					24 packets per day				
Node Number	Packet Number	No ADR	%	ADR	%	Packet Number	No ADR	%	ADR	%
34	4896	4.37	0.09	2.1	0.04	9792	16.53	0.17	8	0.08
68	9792	25.23	0.26	8.63	0.09	19584	98.27	0.5	29.63	0.15
102	14688	57.43	0.39	15.77	0.11	29376	231.53	0.79	52.5	0.18
136	19584	113.63	0.58	28.2	0.14	39168	461.9	1,18	89.3	0.23
170	24480	181.67	0.74	47.57	0.19	48960	722,23	1.48	140.7	0.29
	48 packets per day					96 packets per day				
Node Number	Packet Number	No ADR	%	ADR	%	Packet Number	No ADR	%	ADR	%
34	19584	63.53	0.32	27.17	0.14	39168	217.93	0.56	107.17	0.27
68	39168	374.43	0.96	107.4	0.27	78336	1321.13	1.69	431.1	0.55
102	58752	847.73	1.44	186.33	0.32	117504	2987.67	2.54	716.57	0.61
136	78336	1687.5	2.15	309.67	0.4	156672	5813.17	3.71	1113.5	0.71
170	97920	2657.9	2.71	470.33	0.48	195840	9144.6	4.67	1671.17	0.85

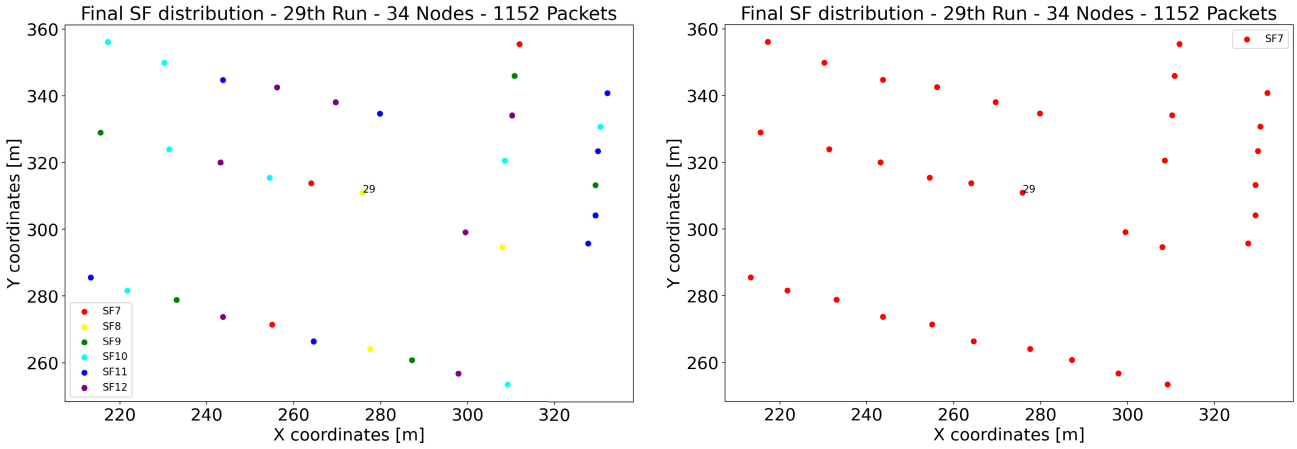

(a) ADR Disabled (b) ADR Enabled

FIGURE 12. SF distribution with 34 nodes sending 1152 packets.

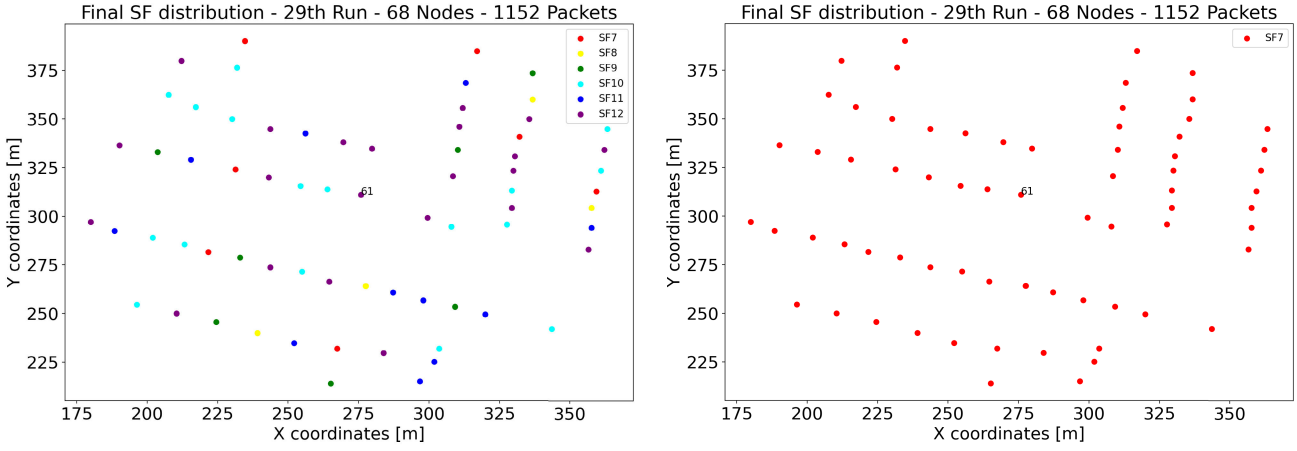

(a) ADR Disabled (b) ADR Enabled

FIGURE 13. SF distribution with 68 nodes sending 1152 packets.

of collisions in ADR-enabled cases are lower with respect to ADR-disabled cases, as can be seen in Table 4. However, when there is a high packet frequency (i.e., 96 packets per day), improvements starts to be noticeable, which can be explained by the continuous evaluation of the ADR mechanism. This will continuously be triggered when

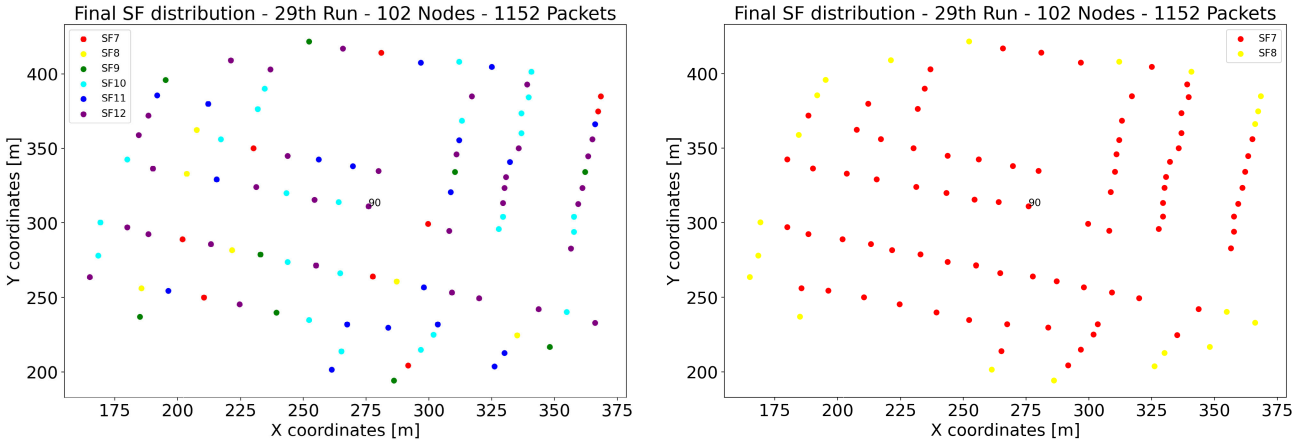

(a) ADR Disabled **(b)** ADR Enabled

FIGURE 14. SF distribution with 102 nodes sending 1152 packets.

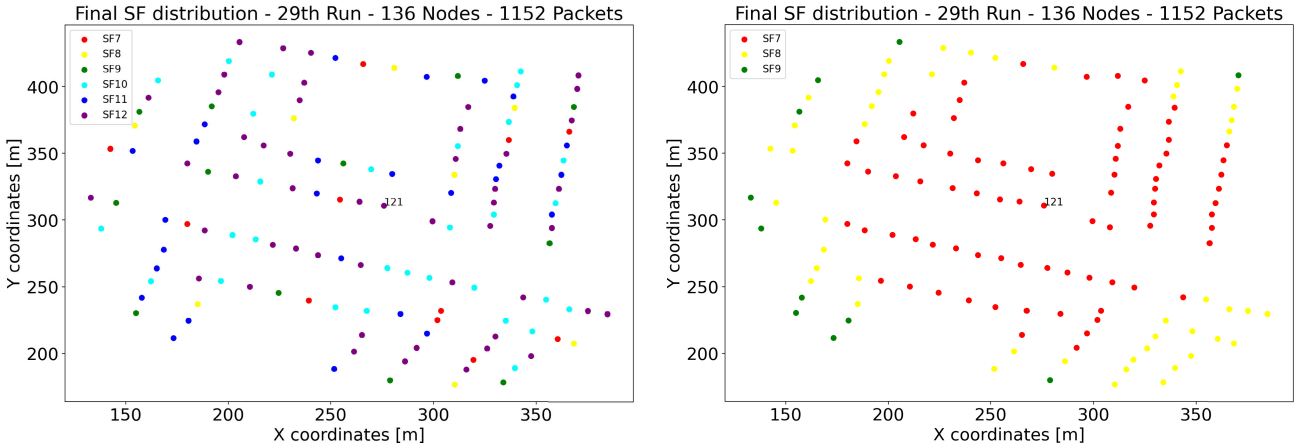

(a) ADR Disabled **(b)** ADR Enabled

FIGURE 15. SF distribution with 136 nodes sending 1152 packets.

$N = 20$ packets are transmitted for every end-device and can cause, in this case, a slight decrease in network performance. A possible improvement is to store the previous network status and operation, so automatically, the network can revert its operation to a previous status where it was operating at an optimal point.

Another point is the number of collisions per case, which is consistent with the transmitted packet frequency. However, when networks operate with ADR-disabled and considering a high packet frequency (i.e., 96 packets per day), several collisions occur owing to static network operation, regarding the operating frequency of devices and transmission power. Even when the packet frequency is low (i.e., 12 and 24 packets per day), networks with ADR-enabled tend to perform better, nonetheless, at the expense of having a slightly lower delivery ratio.

The conclusion from this point is that networks with ADR mechanism enabled tend to have an overall better performance considering collisions, reception throughput, and energy consumption, at the expense of a slightly lower delivery ratio. Indeed, these facts are trade-offs that must be taken into consideration by network engineers in terms of how much margins are the requirements for giving importance to specific metrics.

G. SF DISTRIBUTION

This section analyzes and comments on the distribution of SF in the neighborhood area, comparing results with and without ADR, and how the effect of more transmitted packets is reflected in the final distribution. We chose the distribution result of the 29th run in each case, as it is one of the 30 executed runs. The chosen scenario is when nodes communicate with the network server every 15 min, as this is the scenario where changes can be seen due to more transmitted packets, and causing more iterations of the ADR mechanisms. Figures 12 to 16 show the differences between ADR enabled

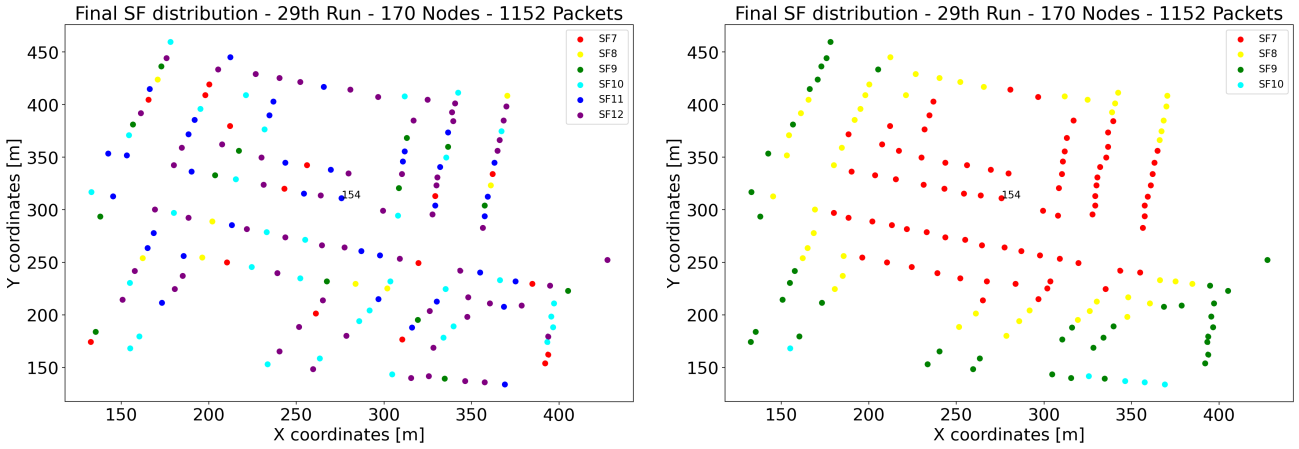

(a) ADR Disabled (b) ADR Enabled

FIGURE 16. SF distribution with 170 nodes sending 1152 packets.

and disabled in the considered suburban neighborhood. It is essential to note that the LoRa gateway (LoRa-GW) node is located where a number mark is drawn, differentiating it from other nodes (i.e., end-devices or SMs).

The simulation results show that when the ADR mechanism is disabled, no SF change is taken in the network, resulting in every node having its initial SF value. As these are generated randomly, a diverse distribution is expected in every case regarding the size. However, when activating ADR mechanisms, the difference was noticeable at the first moment. When there are a small number of nodes (e.g., 34 or 68 nodes), every node has the same spreading factor when communication is almost constant with the network server (every node sends packets every 15 min). The mentioned behavior is shown in Figs. 12 and 13.

On the other hand, when the number of nodes increases, different SF values start to increase. When 102 nodes are present, two SFs occur, meaning that the need for different transmission windows or frequencies is present at this point in node numbers. Delivery ratio values can be considered the same; therefore, this mechanism helps to maintain and upgrade the network conditions. Final scenarios with a higher number of nodes translate into more diversity in the SF values, as presented in Figs. 14, 15, and 16.

From the above results, with ADR enabled, it is worth mentioning that SMs near the LoRaGW are assigned to a lower SF value (i.e., higher data rates can be achievable), while far-located devices have higher SF values (lower data rates) in order to maintain link quality given geographical conditions. This result is validated by the analyzes given in the state-of-the-art results, where nodes near the gateway have the best data rates, whereas far-located devices have the opposite case. Under these circumstances, the proposed architecture and communication schemes can serve as future IoT-based network for AMI in suburban neighborhoods.

VII. CONCLUSION

This paper proposed an IoT-based architecture for AMI networks, which is a key component for deploying the future smart grid concept. A particular case of LoRa communication technology is considered as a promising candidate for deploying the proposed architecture. Several aspects are discussed regarding physical layer characteristics, media access control (MAC) layer characteristics, and the importance of ADR mechanism for dynamic behavior and scalable LoRa networks. A simulation scenario of the AMI system was considered for a suburban neighborhood. Several aspects are discussed and evaluated to determine if LoRa technology can be operated under different circumstances. The simulation results were compared considering two different operation scenarios of LoRa networks under various metrics, such as delivery ratio, energy consumption, throughput, collisions, and SF distribution. The proposed solution was used to deploy the smart meters in an AMI network and enables the network to be dynamic and solve scalability issues in future configurations (adding more smart meters). Future work aims to extend the current simulation model to support multiple gateways in a neighborhood area network. Furthermore, the actual implementation of the LoRa network on the university campus is in progress, and the results of the LoRa implementation will be compared with the simulation results.

REFERENCES

[1] W. Luan, D. Shart, and S. Lancashire, "Smart grid communication network capacity planning for power utilities," in *Proc. IEEE PES T&D*, New Orleans, LA, USA, Apr. 2010, pp. 1–4, doi: 10.1109/TDC.2010.5484223.
[2] F. E. Abrahamsen, Y. Ai, and M. Cheffena, "Communication technologies for smart grid: A comprehensive survey," 2021, *arXiv:2103.11657*. [Online]. Available: http://arxiv.org/abs/2103.11657
[3] W. Luan, D. Sharp, and S. LaRoy, "Data traffic analysis of utility smart metering network," in *Proc. IEEE Power Energy Soc. Gen. Meeting*, Jul. 2013, pp. 1–4, doi: 10.1109/PESMG.2013.6672750.
[4] M. I. Nashiruddin and A. A. F. Purnama, "NB-IoT network planning for advanced metering infrastructure in Surabaya, Sidoarjo, and Gresik," in *Proc. 8th Int. Conf. Inf. Commun. Technol. (ICoICT)*, Jun. 2020, pp. 1–6, doi: 10.1109/ICoICT49345.2020.9166315.

[5] Y. Bagariang, M. I. Nashiruddin, and N. Mufti Adriansyah, "LoRa-based IoT network planning for advanced metering infrastructure in urban, suburban and rural scenario," in *Proc. Int. Seminar Res. Inf. Technol. Intell. Syst. (ISRITI)*, Dec. 2019, pp. 1–6, doi: 10.1109/ISRITI48646.2019.9034583.

[6] *AMI in Review: Informing the Conversation*, Office of Electricity US Department of Energy, Washington, DC, USA, Aug. 2020, pp. 1–34. Accessed: Jul. 11, 2021.

[7] D. Bian, M. Kuzlu, M. Pipattanasomporn, S. Rahman, and D. Shi, "Performance evaluation of communication technologies and network structure for smart grid applications," *IET Commun.*, vol. 13, no. 8, pp. 1025–1033, 2019, doi: 10.1049/iet-com.2018.5408.

[8] A. Sahu, A. Goulart, and K. Butler-Purry, "Modeling AMI network for real-time simulation in NS-3," in *Proc. Princ., Syst. Appl. IP Telecommun. (IPTComm)*, Oct. 2016, pp. 1–8, doi: 10.1109/IPTComm39427.2016.7780248.

[9] Y. Zhang, W. Sun, L. Wang, H. Wang, R. C. Green, and M. Alam, "A multilevel communication architecture of smart grid based on congestion aware wireless mesh network," in *Proc. North Amer. Power Symp.*, Aug. 2011, pp. 1–6, doi: 10.1109/NAPS.2011.6025169.

[10] D. Bian, M. Kuzlu, M. Pipattanasomporn, and S. Rahman, "Analysis of communication schemes for advanced metering infrastructure (AMI)," in *Proc. IEEE PES Gen. Meeting Conf. Expo.*, Jul. 2014, pp. 1–5, doi: 10.1109/PESGM.2014.6939562.

[11] N. Saputro and K. Akkaya, "Investigation of smart meter data reporting strategies for optimized performance in smart grid AMI networks," *IEEE Internet Things J.*, vol. 4, no. 4, pp. 894–904, Aug. 2017, doi: 10.1109/JIOT.2017.2701205.

[12] C.-C. Sun, D. J. Sebastian Cardenas, A. Hahn, and C.-C. Liu, "Intrusion detection for cybersecurity of smart meters," *IEEE Trans. Smart Grid*, vol. 12, no. 1, pp. 612–622, Jan. 2021, doi: 10.1109/TSG.2020.3010230.

[13] A. Rahman and M. Suryanegara, "The development of IoT LoRa: A performance evaluation on LoS and non-LoS environment at 915 MHz ISM frequency," in *Proc. Int. Conf. Signals Syst. (ICSigSys)*, May 2017, pp. 1–5, doi: 10.1109/ICSIGSYS.2017.7967033.

[14] Y. Ishida, D. Nobayashi, and T. Ikenaga, "Experimental performance evaluation of the collisions in LoRa communications," in *Proc. Int. Conf. Comput. Sci. Comput. Intell. (CSCI)*, Dec. 2018, pp. 1–4, doi: 10.1109/CSCI46756.2018.00200.

[15] *IT/OT Convergence Issue Brief*, Issue Brief, Utilities Technology Council (UTC), Richmond, VA, USA, Jul. 2017, pp. 1–2. Accessed: Jul. 7, 2021.

[16] B. Karimi and V. Namboodiri, "Capacity analysis of a wireless backhaul for metering in the smart grid," in *Proc. IEEE INFOCOM Workshops*, Mar. 2012, pp. 1–6, doi: 10.1109/INFCOMW.2012.6193520.

[17] R. Berthier, D. I. Urbina, A. A. Cardenas, M. Guerrero, U. Herberg, J. G. Jetcheva, D. Mashima, J. H. Huh, and R. B. Bobba, "On the practicality of detecting anomalies with encrypted traffic in AMI," in *Proc. IEEE Int. Conf. Smart Grid Commun. (SmartGridComm)*, Nov. 2014, pp. 1–6, doi: 10.1109/SmartGridComm.2014.7007761.

[18] C. Karupongsiri, K. S. Munasinghe, and A. Jamalipour, "Smart meter packet transmission via the control signal of LTE networks," in *Proc. IEEE Int. Conf. Commun. (ICC)*, Jun. 2015, pp. 1–6, doi: 10.1109/ICC.2015.7248782.

[19] N. Andreadou, E. Kotsakis, and M. Masera, "Smart meter traffic in a real LV distribution network," *Energies*, vol. 11, no. 5, pp. 1–27, May 2018, doi: 10.3390/en11051156.

[20] S. A. Salam, S. A. Mahmud, G. M. Khan, and H. S. Al-Raweshidy, "M2M communication in smart grids: Implementation scenarios and performance analysis," in *Proc. IEEE Wireless Commun. Netw. Conf. Workshops (WCNCW)*, Apr. 2012, pp. 1–6, doi: 10.1109/WCNCW.2012.6215478.

[21] Z. Qin, Y. Shenglong, Z. Heng, C. Xuesheng, Z. Shengmao, and D. Yang, "Design and implementation of marine temperature measurement system based on LoRa," in *Proc. Int. Symp. Sens. Instrum. IoT Era (ISSI)*, Sep. 2018, pp. 1–4, doi: 10.1109/ISSI.2018.8538213.

[22] M. Rizzi, P. Ferrari, A. Flammini, and E. Sisinni, "Evaluation of the IoT LoRaWAN solution for distributed measurement applications," *IEEE Trans. Instrum. Meas.*, vol. 66, no. 12, pp. 3340–3349, Dec. 2017, doi: 10.1109/TIM.2017.2746378.

[23] G. M. Bianco, A. Mejia-Aguilar, and G. Marrocco, "Performance evaluation of LoRa LPWAN technology for mountain search and rescue," in *Proc. 5th Int. Conf. Smart Sustain. Technol. (SpliTech)*, Sep. 2020, pp. 1–4, doi: 10.23919/SpliTech49282.2020.9243817.

[24] M. O. Ojo, D. Adami, and S. Giordano, "Network performance evaluation of a LoRa-based IoT system for crop protection against ungulates," in *Proc. IEEE 25th Int. Workshop Comput. Aided Modeling Design Commun. Links Netw. (CAMAD)*, Sep. 2020, pp. 1–6, doi: 10.1109/CAMAD50429.2020.9209317.

[25] K. Mikhaylov, J. Petajajarvi, and T. Hanninen, "Analysis of capacity and scalability of the LoRa low power wide area network technology," in *Proc. 22th Eur. Wireless Conf. Eur. Wireless*, Oulu, Finland, May 2016, pp. 1–6.

[26] M. C. Bor, U. Roedig, T. Voigt, and J. M. Alonso, "Do LoRa low-power wide-area networks scale?" in *Proc. 19th ACM Int. Conf. Modeling, Anal. Simulation Wireless Mobile Syst.*, Nov. 2016, pp. 1–9, doi: 10.1145/2988287.2989163.

[27] S. Abboud, N. el Rachkidy, A. Guitton, and H. Safa, "Gateway selection for downlink communication in LoRaWAN," in *Proc. IEEE Wireless Commun. Netw. Conf. (WCNC)*, Apr. 2019, pp. 1–6, doi: 10.1109/WCNC.2019.8885756.

[28] A. Al-Fuqaha, M. Guizani, M. Mohammadi, M. Aledhari, and M. Ayyash, "Internet of Things: A survey on enabling technologies, protocols, and applications," *IEEE Commun. Surveys Tuts.*, vol. 17, no. 4, pp. 2347–2376, 4th Quart., 2015, doi: 10.1109/COMST.2015.2444095.

[29] I. Worighi, A. Maach, and A. Hafid, "Smart grid architecture and impact analysis of a residential microgrid," in *Proc. 4th IEEE Int. Colloq. Inf. Sci. Technol. (CiSt)*, Oct. 2016, pp. 1–6, doi: 10.1109/CIST.2016.7805008.

[30] M. A. Ahmed, A. M. Eltamaly, M. A. Alotaibi, A. I. Alolah, and Y.-C. Kim, "Wireless network architecture for cyber physical wind energy system," *IEEE Access*, vol. 8, pp. 40180–40197, 2020, doi: 10.1109/ACCESS.2020.2976742.

[31] S. M. A. A. Abir, A. Anwar, J. Choi, and A. S. M. Kayes, "IoT-enabled smart energy grid: Applications and challenges," *IEEE Access*, vol. 9, pp. 50961–50981, 2021, doi: 10.1109/ACCESS.2021.3067331.

[32] Y. Yongyong and H. Chenghao, "Design of data acquisition system of electric meter based on ZigBee wireless technology," in *Proc. IEEE Int. Conf. Adv. Electr. Eng. Comput. Appl. (AEECA)*, Aug. 2020, pp. 1–4, doi: 10.1109/AEECA49918.2020.9213519.

[33] J.-D. Jeong, Y. Shin, and I.-W. Lee, "Long-range transmission of photovoltaic climate information through the LoRa radio," in *Proc. Int. Conf. Inf. Commun. Technol. Converg. (ICTC)*, Oct. 2018, pp. 1–4, doi: 10.1109/ICTC.2018.8539429.

[34] L. Wan, Z. Zhang, and J. Wang, "Demonstrability of narrowband Internet of Things technology in advanced metering infrastructure," *EURASIP J. Wireless Commun. Netw.*, vol. 2019, no. 1, pp. 1–12, Dec. 2019, doi: 10.1186/s13638-018-1323-y.

[35] "LoRa and LoRaWAN: A technical overview," Semtech Corporation, Camarillo, CA, USA, Tech. Rep. Dec. 2019, pp. 1–26. Accessed: Jul. 7, 2021. [Online]. Available: https://lora-developers.semtech.com/uploads/documents/files/LoRa_and_LoRaWAN-A_Tech_Overview-Downloadable.pdf

[36] H. Mroue, A. Nasser, B. Parrein, S. Hamrioui, E. Mona-Cruz, and G. Rouyer, "Analytical and simulation study for LoRa modulation," in *Proc. 25th Int. Conf. Telecommun. (ICT)*, Jun. 2018, pp. 1–5, doi: 10.1109/ICT.2018.8464879.

[37] B. Dunlop, H. H. Nguyen, R. Barton, and J. Henry, "Interference analysis for LoRa chirp spread spectrum signals," in *Proc. IEEE Can. Conf. Electr. Comput. Eng. (CCECE)*, May 2019, pp. 1–5, doi: 10.1109/CCECE.2019.8861956.

[38] B. Reynders and S. Pollin, "Chirp spread spectrum as a modulation technique for long range communication," in *Proc. Symp. Commun. Veh. Technol. (SCVT)*, Nov. 2016, pp. 1–5, doi: 10.1109/SCVT.2016.7797659.

[39] A. Augustin, J. Yi, T. Claussen, and W. M. Townsley, "A study of LoRa: Long range & low power networks for the Internet of Things," *Sensors*, vol. 16, no. 9, p. 1466, 2016.

[40] J. Finnegan, R. Farrell, and S. Brown, "Analysis and enhancement of the LoRaWAN adaptive data rate scheme," *IEEE Internet Things J.*, vol. 7, no. 8, pp. 7171–7180, Aug. 2020, doi: 10.1109/JIOT.2020.2982745.

[41] T. Watteyne, A. Mehta, and K. Pister, "Reliability through frequency diversity: Why channel hopping makes sense," in *Proc. 6th ACM Symp. Perform. Eval. Wireless Ad Hoc, Sensor, Ubiquitous Netw. (PE-WASUN)*, 2009, pp. 1–8, doi: 10.1145/1641876.1641898.

[42] K. Staniec and M. Kowal, "LoRa performance under variable interference and heavy-multipath conditions," *Wireless Commun. Mobile Comput.*, vol. 2018, pp. 1–10, Apr. 2018, doi: 10.1155/2018/6931083.

[43] B. Reynders, W. Meert, and S. Pollin, "Range and coexistence analysis of long range unlicensed communication," in *Proc. 23rd Int. Conf. Telecommun. (ICT)*, May 2016, pp. 1–6, doi: 10.1109/ICT.2016.7500415.

[44] R. Kufakunesu, G. P. Hancke, and A. M. Abu-Mahfouz, "A survey on adaptive data rate optimization in LoRaWAN: Recent solutions and major challenges," *Sensors*, vol. 20, no. 18, p. 5044, Sep. 2020, doi: 10.3390/s20185044.
[45] *LoRaWAN Specification*, Protocol Description, LoRa Alliance, Fremont, CA, USA, Jan. 2015, pp. 1–82. Accessed: Jul. 10, 2021.
[46] M. Slabicki, G. Premsankar, and M. Di Francesco, "Adaptive configuration of LoRa networks for dense IoT deployments," in *Proc. NOMS IEEE/IFIP Netw. Oper. Manage. Symp.*, Apr. 2018, pp. 1–9, doi: 10.1109/NOMS.2018.8406255.
[47] J. L. Gallardo, M. A. Ahmed, and N. Jara, "Clustering algorithm-based network planning for advanced metering infrastructure in smart grid," *IEEE Access*, vol. 9, pp. 48992–49006, 2021, doi: 10.1109/ACCESS.2021.3068752.

JOSÉ LUIS GALLARDO is currently pursuing the M.Sc. degree in electronics engineering (telematics specialization) from Universidad Técnica Federico Santa María (UTFSM), Chile. His current research interests include smart grids, network planning, and data mining.

MOHAMED A. AHMED received the B.Sc. and M.Sc. degrees in electrical engineering (electronics and communications) from Minia University, Minia, Egypt, in 2003 and 2007, respectively, and the Ph.D. degree in electronics and information engineering from Chonbuk National University, Jeonju, South Korea, in 2014. He is currently working as an Assistant Professor with the Department of Electronic Engineering, Universidad Técnica Federico Santa María (UTFSM), Chile, and the Department of Communications and Electronics, Higher Institute of Engineering and Technology–King Marriott, Alexandria, Egypt. Prior to joining UTFSM, he worked as a Postdoctoral Research Fellow at the Advanced Communication and Network Laboratory (ADCAN), Chonbuk National University, from 2014 to 2018. His research interests include wireless sensor networks, wind energy, electric vehicles, smart grid, and cyber-physical systems.

NICOLÁS JARA (Member, IEEE) received the B.Sc. and M.Sc. degrees in telematics engineering from Universidad Técnica Federico Santa María (UTFSM), Chile, in 2010, and the Ph.D. degree on a double graduation program between Université de Rennes I, France, and UTFSM, in 2017 and 2018, respectively. He is currently an Assistant Professor with the Department of Electronics Engineering, UTFSM. His current research interests include optical network design, network performability, and simulation techniques.